Chapter 13
Essentially Non-periodic Processes

This chapter describes a possible physical basis for NSTT in case of essentially non-periodic processes. The physical time is structured to match the one-dimensional dynamics of rigid-body chain of identical particles. Namely, the continuous "global" time is associated with the propagation of linear momentum, whereas a sequence of nonsmooth "local" times describe behaviors of individual physical particles. Such an idea helps to incorporate temporal symmetries of the dynamics into differential equations of motion in many other cases of regular or irregular sequences of internal impacts or external pulses. Since the local times are bounded, a much wider set of analytical tools becomes possible, whereas matching conditions are generated automatically by the corresponding time substitution.

13.1 Nonsmooth Time Decomposition and Pulse Propagation in a Chain of Particles

The periodic version of NSTT employs basis functions generated by the most simple impact oscillator. This is based on the fact that the triangle and square waves capture general temporal symmetries of periodic processes regardless specifics of individual vibrating systems. Below, a non-periodic pair of nonsmooth functions is considered, such as the ramp function,

$$s\,(t;d) = \frac{1}{2}\,(d + |t| - |t-d|) \tag{13.1}$$

and its first-order generalized derivative, $\dot{s}\,(t;d)$, with respect to the temporal argument, t; see Figs. 13.1 and 13.2, respectively.

Such kind of functions play an important role in signal analyses [98].

V. N. Pilipchuk, *Oscillators and Oscillatory Signals from Smooth to Discontinuous*,
https://doi.org/10.1007/978-3-031-37788-4_13

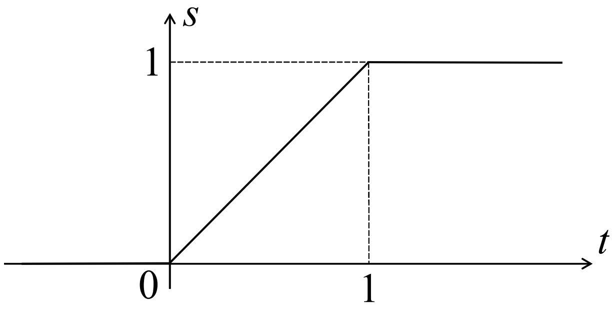

Fig. 13.1 The unit slope ramp function at $d = 1.0$

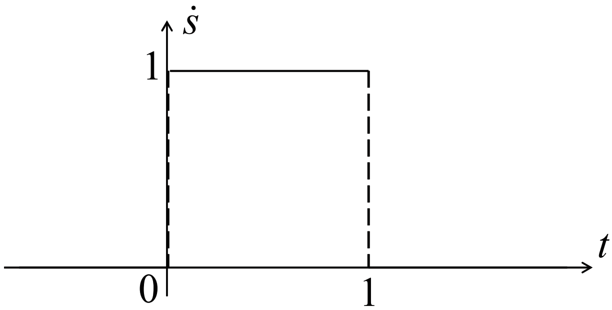

Fig. 13.2 First derivative of the ramp function

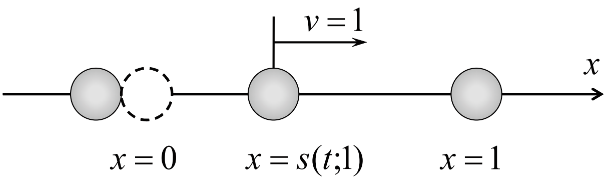

Fig. 13.3 Physical meaning of the ramp function: $s(t;\, 1)$ describes position of the bead struck by another bead from the left and moving until it strikes the next bead of the same mass

Possible physical interpretation of these functions is represented in Fig. 13.3. Namely, the function $s\,(t, d)$ can be treated as a coordinate of a particle, say a very small perfectly stiff bead, initially located at the origin $x = 0$. At the time instance $t = 0$, this bead is struck by the identical bead with the velocity $v = 1$. After the linear momentum exchange, the reference bead starts moving until it stopped by the third bead $x = d$; in our case $d = 1$.

Now, let us consider an infinite chain of the identical perfectly stiff beads located regularly on a straight line at the points x_i $(i = 0, 1, \ldots)$. No energy loss is assumed so that any currently moving bead has the same velocity. As a result, the linear momentum is translated with the constant speed $v = 1$, whereas the beads are interacting at the time instances $t_i = x_i$. Making the temporal shift $t \to t - t_i$ in function (13.1) gives

$$s_i(t) = s(t - t_i, d_i) = \frac{1}{2}(d_i + |t - t_i| - |t - t_{i+1}|) \tag{13.2}$$

where $d_i = t_{i+1} - t_i$.

Due to the unit velocity, function (13.2) can play the role of "local" time for the bead moving within the interval $x_i < x < x_{i+1}$ during the "global" time interval $t_i < t < t_{i+1}$. The term "local" means that the temporal variable s_i starts at zero when the "global" time, t, has reached the point $t = t_i$.

In other words, *the global temporal variable is associated with the linear momentum, whereas all the local temporal variables are attached to the physical bodies.*

For any sequence of time instances, $\Lambda = \{t_0, t_1, \ldots\}$, the global time, $t \in (t_0, \infty)$, can be expressed through the sequence of local times, $\{s_i\}$, as

$$t = \sum_{i=0}^{\infty}(t_i + s_i)\dot{s}_i \tag{13.3}$$

where the derivatives $\dot{s}_i$ satisfy the relationship

$$\dot{s}_i\dot{s}_j = \dot{s}_i\delta_{ij} \tag{13.4}$$

Practically, equality (13.3) is always a finite sum because temporal intervals of physical processes always have finite upper bounds. This equality can be verified analytically within an arbitrary interval, $t_i < t < t_{i+1}$, by means of definitions (13.1) and (13.2), although its geometrical meaning is quite clear from the graphs of participating functions. Formally differentiating both sides of equality (13.3) with respect to t and taking into account (13.4) give

$$1 = \sum_{i=0}^{\infty}\dot{s}_i + t_0\delta(t - t_0) \tag{13.5}$$

Hence,

$$\sum_{i=0}^{\infty}\dot{s}_i = 1 \qquad (t > t_0) \tag{13.6}$$

Equality (13.6) holds based on the definition for $\dot{s}_i$ as illustrated in Fig. 13.2. Note that the right-hand side of expansion (13.3) can be viewed as an element of algebra with the orthogonal basis $\{s_i\}$ and multiplication rule (13.4). This significantly eases different manipulations with the temporal variable (13.3), for instance,

$$t^n = \sum_{i=0}^{\infty} (t_i + s_i)^n \dot{s}_i, \quad n = 1, 2, ... \tag{13.7}$$

or, generally,

$$x(t) = \sum_{i=0}^{\infty} x(t_i + s_i)\dot{s}_i \equiv \sum_{i=0}^{\infty} X_i(s_i)\dot{s}_i \tag{13.8}$$

Since the right-hand sides of (13.7) and (13.8) have the same structure as the argument t itself, then the following functional linearity holds for a general function g

$$g\left(\sum_{i=0}^{\infty} X_i \dot{s}_i\right) = \sum_{i=0}^{\infty} g(X_i)\dot{s}_i \tag{13.9}$$

Now, differentiating (13.8) with respect to time t, and taking into account that $s_i(t_i) = 0$ and $s_{i-1}(t_i) = d_{i-1}$, gives

$$\begin{aligned} \dot{x}(t) &= \sum_{i=0}^{\infty} X_i'(s_i)\dot{s}_i + \sum_{i=0}^{\infty} X_i(s_i)[\delta(t - t_i) - \delta(t - t_{i+1})] \\ &= \sum_{i=0}^{\infty} X_i'(s_i)\dot{s}_i + \sum_{i=0}^{\infty} [X_i(0) - X_{i-1}(d_{i-1})]\delta(t - t_i) \end{aligned} \tag{13.10}$$

where $X_{-1}(d_{-1}) = 0$.

Therefore, all the δ—functions are eliminated from (13.10) under condition, which can be qualified as a necessary condition of continuity for $x(t)$

$$X_i(0) - X_{i-1}(d_{i-1}) = 0 \tag{13.11}$$

Under condition (13.11), the derivative $\dot{x}(t)$ has the same algebraic structure as the function $x(t)$ itself. As a result, transformation (13.3) can be applied to a general class of dynamical systems. Moreover, in the case of impulsively loaded systems, the sequences of δ-functions in (13.10) can be utilized for eliminating the corresponding singularities from dynamical systems.

13.2 Impulsively Loaded Dynamical Systems

Let us consider a dynamical system subjected to an arbitrary sequence of impulses, applied to the system at time instances $\Lambda = \{t_0, t_1, \ldots\}$,

$$\dot{\mathbf{x}} = \mathbf{f}(\mathbf{x}, t) + \sum_{i=0}^{\infty} \mathbf{p}_i \delta(t - t_i), \qquad \mathbf{x}(t) \in R^n \tag{13.12}$$

$$\mathbf{x} \equiv 0, \qquad t < t_0 \tag{13.13}$$

where $\mathbf{f}(\mathbf{x}, t)$ is a sufficiently smooth vector-function and $\mathbf{p}_i$ is vector characterizing magnitudes and directions of the impulses.

In particular case, when $t_0 = 0$, and $\mathbf{p}_i = \mathbf{0}$ $(i = 1, \ldots)$, systems (13.12) and (13.13) become equivalent to the following initial value problem

$$\dot{\mathbf{x}} = \mathbf{f}(\mathbf{x}, t), \qquad \mathbf{x}(0) = \mathbf{p}_0 \tag{13.14}$$

Below, solution of the initial value problem (13.12) and (13.13) is introduced in the specific form based on the operator Lie associated with dynamical system (13.14)

$$\begin{aligned} A &= \mathbf{f}(\mathbf{x}, t)\frac{\partial}{\partial \mathbf{x}} + \frac{\partial}{\partial t} \\ &= f_1(\mathbf{x}, t)\frac{\partial}{\partial x_1} + \ldots. + f_n(\mathbf{x}, t)\frac{\partial}{\partial x_n} + \frac{\partial}{\partial t} \end{aligned} \tag{13.15}$$

It is known, for instance, that the exponent of operator (13.15) produces temporal shifts as follows

$$\begin{aligned} e^{zA}\mathbf{f}(\mathbf{x}(t), t) &= \mathbf{f}(\mathbf{x}(t+z), t+z) \\ &= \mathbf{f}(\mathbf{x}, t) + \left[\mathbf{f}(\mathbf{x}, t)\frac{\partial \mathbf{f}(\mathbf{x}, t)}{\partial \mathbf{x}} + \frac{\partial(\mathbf{x}, t)}{\partial t}\right] z + O(z^2) \end{aligned} \tag{13.16}$$

Proposition 13.2.1 *Solution of the initial value problem (13.12) and (13.13) can be represented in the form*

$$\mathbf{x}(t) = \sum_{i=0}^{\infty} [\mathbf{a}_{i-1} + \mathbf{p}_i + \mathbf{F}(\mathbf{a}_{i-1} + \mathbf{p}_i, t_i, s_i(t))]\, \dot{s}_i(t) \tag{13.17}$$

where $\mathbf{a}_i = \mathbf{x}(t_{i+1})$ *is the sequence of constant vectors determined by the mapping*

$$\begin{aligned} &\mathbf{a}_{-1} = 0 \\ &\mathbf{a}_i = \mathbf{a}_{i-1} + \mathbf{p}_i + \mathbf{F}(\mathbf{a}_{i-1} + \mathbf{p}_i, t_i, d_i); \qquad i = 1, 2, \ldots \end{aligned} \tag{13.18}$$

and the function F *is defined by*

$$\mathbf{F}(\mathbf{x}, t, z) = \int_0^z e^{zA}\mathbf{f}(\mathbf{x}, t)\, dz \tag{13.19}$$

where A *is the operator Lie (13.15).*

Proof Substituting vector analogs of expressions (13.8), and (13.10) into the differential equation of motion (13.12) and taking into account (13.9) give

$$\sum_{i=0}^{\infty}\{[\mathbf{X}_i'(s_i) - \mathbf{f}(\mathbf{X}_i(s_i), t_i + s_i)]\dot{s}_i +$$

$$[\mathbf{X}_i(0) - \mathbf{X}_{i-1}(d_{i-1}) - \mathbf{p}_i]\delta(t - t_i)\} = 0 \tag{13.20}$$

The left-hand side of expression (13.20) includes both regular and singular terms. Moreover, the basis elements $\dot{s}_i$ are linearly independent, and all the δ-functions are acting at different time instances. Therefore, Eq. (13.20) gives

$$\mathbf{X}_i'(s_i) = \mathbf{f}(\mathbf{X}_i(s_i), t_i + s_i) \tag{13.21}$$

$$\mathbf{X}_i(0) = \mathbf{X}_{i-1}(d_{i-1}) + \mathbf{p}_i = \mathbf{a}_{i-1} + \mathbf{p}_i \tag{13.22}$$

where $\mathbf{a}_{-1} = 0$ and $\mathbf{a}_i = \mathbf{X}_i(d_i)$ $(i = 0, 1, 2, ...)$. Equation (13.21) can be represented in the integral form

$$\mathbf{X}_i(s_i) = \mathbf{X}_i(0) + \int_0^{s_i} \mathbf{f}(\mathbf{X}_i(z), t_i + z)\, dz \tag{13.23}$$

Since the variable of integration is limited by the interval $0 \le z \le s_i$, the integrand in (13.23) can be approximated by the easy to integrate Maclaurin's series with respect to z. Moreover, such a series can be represented in the convenient form of Lie series based on the fact that $\mathbf{X}_i(z)$ are coordinates of the dynamical system with the operator Lie (13.15). As a result, all the coefficients of power series are expressed through the "initial conditions" at $z = 0$ $(t = t_i)$ by enforcing the form of the dynamical system. As a result, no high-order derivatives of the coordinates are included anymore into the coefficients of the series. Taking into account the notation $\mathbf{X}_i(s_i) = \mathbf{x}(t_i + s_i)$, and expressions (13.16) and (13.19), brings (13.23) to the form

$$\begin{aligned}\mathbf{X}_i(s_i) &= \mathbf{X}_i(0) + \int_0^{s_i} e^{zA}\mathbf{f}(\mathbf{x}(t_i), t_i)\, dz \\ &= \mathbf{X}_i(0) + \mathbf{F}(\mathbf{x}(t_i), t_i, s_i) \\ &= \mathbf{X}_i(0) + \mathbf{F}(\mathbf{X}_i(0), t_i, s_i)\end{aligned} \tag{13.24}$$

Substituting now $\mathbf{X}_i(0)$ from (13.22) in (13.24) gives

$$\mathbf{X}_i(s_i) = \mathbf{a}_{i-1} + \mathbf{p}_i + \mathbf{F}(\mathbf{a}_{i-1} + \mathbf{p}_i, t_i, s_i) \tag{13.25}$$

Finally, substituting (13.25) in expansion (13.8) gives (13.17). Then, substituting $s_i = d_i$ in (13.25) gives (13.18) and thus completes the proof.

Solutions (13.17) and (13.18) should be viewed as a semi-analytic solution, since some numerical tool is required for calculating the discrete mapping (13.18). The central role here belongs to the function $s(t; d)$ (13.1), which is automatically matching all the neighboring pieces of the solution. Note that the distances d_i between times Λ are not necessary small; however, the precision of the solution can be improved by increasing the number of terms of the Lie series $e^{zA}\mathbf{f}(\mathbf{x}, t)$ with respect to z, rather than reducing the distances d_i.

13.2.1 Harmonic Oscillator Under Sequential Impulses

In order to estimate precision of the above procedure, let us consider the particular case in which function (13.19) can be calculated exactly in the closed form due to the presence of exact analytical solution in between the pulses Λ. The differential equation of motion on the entire time range is

$$\ddot{x} + 2\zeta\Omega\dot{x} + \Omega^2 x = \sum_{i=0}^{\infty} p_i \delta(t - t_i) \tag{13.26}$$

In this case, the function $\mathbf{f}(\mathbf{x}, t)$ in Eq. (13.12) becomes

$$\mathbf{f}(\mathbf{x}) = \begin{pmatrix} x_2 \\ -2\zeta\Omega x_2 - \Omega^2 x_1 \end{pmatrix} \tag{13.27}$$

Using the identity $e^{zA}\mathbf{f}(\mathbf{x}(t), t) = \mathbf{f}(\mathbf{x}(t+z), t+z)$ and the exact analytical solution of the corresponding free oscillator gives both components of the vector-function (13.19) in the form

$$\begin{aligned}
F_1(\mathbf{x}; z) &= \left[e^{-z\zeta\Omega} \cos\left(z\sqrt{1-\zeta^2}\,\Omega \right) + \frac{\zeta e^{-z\zeta\Omega}}{\sqrt{1-\zeta^2}} \sin\left(z\sqrt{1-\zeta^2}\,\Omega \right) - 1 \right] x_1 \\
&\quad + \frac{e^{-z\zeta\Omega}}{\Omega\sqrt{1-\zeta^2}} \sin\left(z\sqrt{1-\zeta^2}\,\Omega \right) x_2 \\
F_2(\mathbf{x}; z) &= -\frac{\Omega e^{-z\zeta\Omega}}{\sqrt{1-\zeta^2}} \sin\left(z\sqrt{1-\zeta^2}\,\Omega \right) x_1 \\
&\quad + \left[e^{-z\zeta\Omega} \cos\left(z\sqrt{1-\zeta^2}\,\Omega \right) - \frac{\zeta e^{-z\zeta\Omega}}{\sqrt{1-\zeta^2}} \sin\left(z\sqrt{1-\zeta^2}\,\Omega \right) - 1 \right] x_2
\end{aligned} \tag{13.28}$$

In this particular case, properties of mapping (13.18) depend on the following determinant

$$J = \begin{vmatrix} 1 + \partial F_1/\partial x_1 & \partial F_1/\partial x_2 \\ \partial F_2/\partial x_1 & 1 + \partial F_2/\partial x_2 \end{vmatrix} = e^{-2d_i \zeta \Omega} \tag{13.29}$$

Let us introduce the relative error

$$\delta = \left| J - J_{appr} \right| / J \tag{13.30}$$

where J_{appr} is an approximate determinant based on the Lie series expansion (13.16).

Figures 13.4 and 13.5 show diagrams for the relative error δ versus the distance d between any two neighboring impulse times when the highest-order terms kept in Lie series (13.16) are $O(z^2)$ and $O(z^3)$, respectively.

As follows from the diagrams, precision of the discrete mapping essentially depends on both the distance between pulse times and the number of terms kept in the Lie series. As a result, the error due to a large distance can be reduced by increasing the number of terms in the Lie series.

13.2.2 Random Suppression of Chaos

A specific case of the Duffing oscillator with no linear stiffness under sine modulated random impulses was considered in [183]. The corresponding differential equation of motion is represented in the form

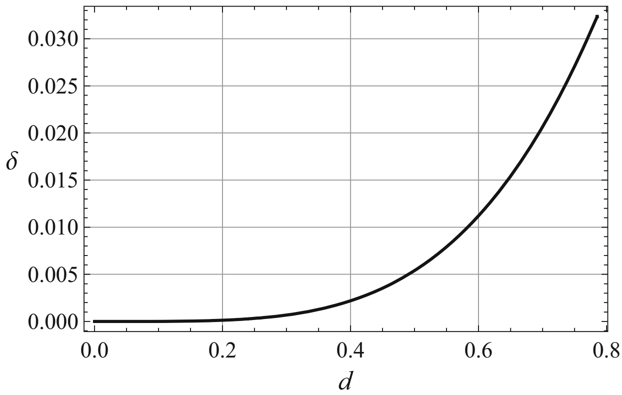

Fig. 13.4 Relative error of the determinant based on the truncated Lie series including terms of order $O(z^2)$

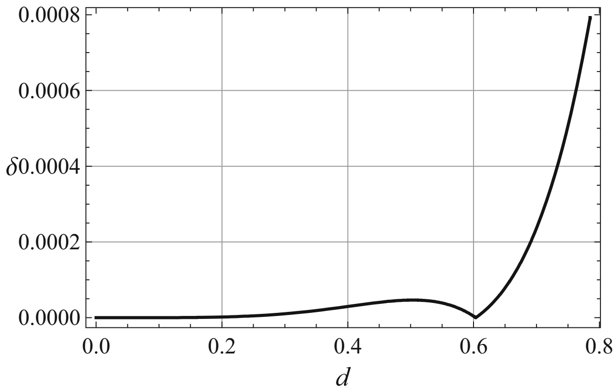

Fig. 13.5 Relative error of the determinant based on the truncated Lie series including terms of order $O(z^3)$

$$\ddot{x} + \zeta \dot{x} + x^3 = B \sin t \sum_{i=0}^{\infty} \delta(t - t_i) \tag{13.31}$$

where ζ is a constant linear damping coefficient and B is the amplitude of modulation.

Distances between any two sequential impulse times are given by

$$d_i = t_{i+1} - t_i = \frac{\pi}{12}\left(1 + \beta \eta_i\right)$$

where η_i is random real number homogeneously distributed on the interval $[-1, 1]$ and β is a small positive number, $0 < \beta \ll 1$.

Introducing the state vector $\mathbf{x} = (x, \dot{x})^T \equiv (x_1, x_2)^T$ brings system (13.31) to the standard form (13.12), where

$$\mathbf{f}(\mathbf{x}) = \begin{pmatrix} x_2 \\ -\zeta x_2 - x_1^3 \end{pmatrix}, \quad \mathbf{p}_i = \begin{pmatrix} 0 \\ B \sin t_i \end{pmatrix}$$

Note that oscillator (13.31) represents of course a modified version of the well-known oscillator, $\ddot{x} + \zeta \dot{x} + x^3 = B \sin t$, considered first by Ueda [236] as a model of nonlinear inductor in electrical circuits—the Ueda circuit. In particular, the result of work [236], as well as many further investigations of similar models, reveals the existence of stochastic attractors often illustrated by the Poincaré diagrams [147]. Similar diagrams obtained under non-regular snapshots can be qualified as "stroboscopic" diagrams. The results of the computer simulations described in [183] show that some irregularity of the pulse times can be used for the purposes of a more clear observation of the system orbits in the stroboscopic diagrams. When repeatedly executing the numerical code, under the same input conditions, such a small disorder in the input results some times in a less noisy and more organized stroboscopic diagrams. However, such phenomenon itself was found to be a random event whose "appearance" depends on the level of pulse randomization as well as the number of iterations.